Biochemical and Biophysical Research Communications 438 (2013) 169–174

Contents lists available at ScienceDirect

Biochemical and Biophysical Research Communications

journal homepage: www.elsevier.com/locate/ybbrc

NMR binding and crystal structure reveal that intrinsically-unstructured regulatory domain auto-inhibits PAK4 by a mechanism different from that of PAK1

Wei Wang [a], Liangzhong Lim [a], Yohendran Baskaran [b], Ed Manser [b], Jianxing Song [a,c,*]

[a] Department of Biological Sciences, Faculty of Science, National University of Singapore, 10 Kent Ridge Crescent, Singapore 119260, Singapore
[b] sGSK Laboratory, Institute of Molecular and Cell Biology, SINGAPORE 138673.
[c] Department of Biochemistry, Yong Loo Lin School of Medicine, National University of Singapore, 10 Kent Ridge Crescent, Singapore 119260, Singapore

ARTICLE INFO

Article history:
Received 11 July 2013
Available online 20 July 2013

Keywords:
p21-activated kinases (PAKs)
Auto-inhibition
Intrinsically unstructured protein (IUP)
Isothermal titration calorimetry (ITC)
NMR spectroscopy
X-ray crystallography

ABSTRACT

Six human PAK members are classified into groups I (PAKs 1–3) and II (PAK4–6). Previously, only group I PAKs were thought to be auto-inhibited but very recently PAK4, the prototype of group II PAKs, has also been shown to be auto-inhibited by its N-terminal regulatory domain. However, the complete auto-inhibitory domain (AID) sequence remains undefined and the mechanism underlying its auto-inhibition is largely elusive. Here, the N-terminal regulatory domain of PAK4 sufficient for auto-inhibiting and binding Cdc42/Rac was characterized to be intrinsically unstructured, but nevertheless we identified the entire AID sequence by NMR. Strikingly, an AID peptide was derived by deleting the binding-unnecessary residues, which has a Kd of 320 nM to the PAK4 catalytic domain. Consequently, the PAK4 crystal structure complexed with the entire AID has been determined, which reveals that the complete kinase cleft is occupied by 20 AID residuescomposed of an N-terminal α-helix and a previously-identified pseudosubstrate motif, thus achieving auto-inhibition. Our study reveals that PAK4 is auto-inhibited by a novel mechanism which is completely different from that for PAK1, thus bearing critical implications for design of inhibitors specific for group II PAKs.

1. Introduction

By direct binding to a variety of "effector" protein kinases including the p21-activated kinases (PAKs), the Rho-family GTPases such as Rac and Cdc42 control many cellular functions, comprisingcytoskeletal organization, morphological change, cell motility, and cell-cycle progression. PAKs function as hubs to interact with multiple partners, and have been demonstrated to be extensively involved in cancer, brain function, and virus infection. In human, the PAK family is composed of six members, which share conserved catalytic and Cdc42/Rac binding (CRIB) domains. They can be further classified into groups I (PAK1, -2, and -3) and II (PAK4, -5, and -6), based on the domain organizations and regulatory properties [1–7]. Previously, only group I PAKs have been demonstrated to be auto-inhibited and activated by Cdc42 or Rac binding. However, very recently PAK4, the prototype of group II PAKs, was also shown to be auto-inhibited by the N-terminal region (20–68) [7]. Moreover, the N-terminal residues 9–68 which are highly conserved in allthree group II PAKs are sufficient for auto-inhibiting PAK4 and binding Cdc42/Rac (Fig. 1A) [7].

Structurally, PAKs share with other non-PAK kinases the core catalytic domain constituted by two subdomains called the kinase lobes, namely N- and C-lobes, in between which is a long cleft called the kinase cleft which accommodates the catalytic machinery including substrate- and ATP-binding pockets [5,8,9]. Previously the crystal structure of the auto-inhibited PAK1 was determined to be a homodimer with each kinase domain bound to an N-terminal auto-inhibitory domain (AID), and consequently the auto-inhibitory mechanism was established [5]. On the other hand, the molecular mechanism underlying theauto-inhibition remains largely elusive for group II PAKs. Only very recently, the determination of PAK4 structures reveals that six residues Arg49-Val54 of the N-terminal regulatory domain are bound to the substrate-binding pocket of the kinase cleft as a pseudosubstrate [9].

However, three key questions remain unanswered for PAK4: 1. what is the solution conformation of the N-terminal regulatory domain in the free state? 2. What is the entire AID sequence? 3. How does the entire AID complex and auto-inhibit the PAK4 catalytic

* Corresponding author at: Department of Biological Sciences, Faculty of Science, National University of Singapore, 10 Kent Ridge Crescent, Singapore 119260, Singapore. Fax: +65 6779 2486.
E-mail address: bchsj@nus.edu.sg (J. Song).

0006-291X/$ - see front matter © 2013 Elsevier Inc. All rights reserved.
http://dx.doi.org/10.1016/j.bbrc.2013.07.047

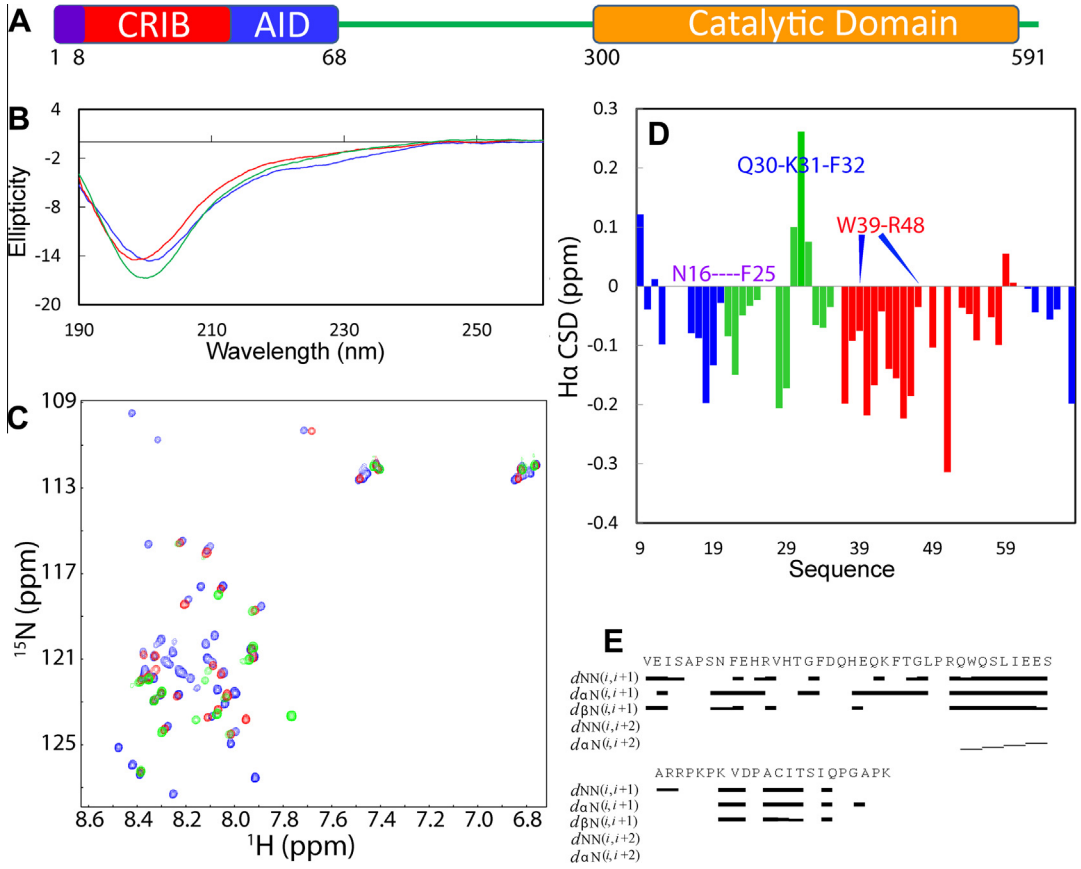

Fig. 1. The N-terminal regulatory domain of PAK4 is predominantly unstructured. (A) Domain organization of PAK4 including the nuclear localization signal over residues 1–8 (NLS, purple), Cdc42/Rac binding (CRIB, red) domain and auto-inhibitory domain (AID, blue) over residues 9–68, as well as catalytic domain (light brown) over residues 300–591. (B) Far-UV CD spectra of three peptides with a protein concentration of 25 μM, over residues 9–68 (blue), 29–61 (red) and 36–60 (green) at 25 °C in 5 mM phosphate buffer (pH 6.3). (C) Two-dimensional ^{1}H–^{15}N NMR HSQC spectra of three peptides with a concentration of 100 μM in 10 mM phosphate buffer (pH 6.3) over residues 9–68 (blue), 29–61 (red) and 36–60 (green) at 25 °C on a Bruker 800 MHz NMR spectrometer. (D) Residue specific Hα chemical shift deviations (CSD) for the full-length regulatory domain (9–68). Green bars are used for representing CRIB residues, red for AID residues, and blue for the rest. (E) NOE connectivity pattern of the full-length regulatory domain (9–68) defining secondary structures. (For interpretation of the references to color in this figure legend, the reader is referred to the web version of this article.)

domain? Here we addressed these questions by a combined use of CD, ITC, NMR spectroscopy and X-ray crystallography.

2. Materials and methods

2.1. Cloning, expression and purification ofproteins

Three peptides (9–68, 29–61, 36–60) derived from the N-terminal regulatory domain of the human PAK4 with the nuclear localization signal (1–8) deleted were cloned into pGEX-4T-1 vector while the human PAK4 catalytic domain was cloned into pSY5M vector. Detailed protocols for protein expression and purification have been described in Supplementary material.

Isotope-labeled proteins for NMR studies were generated as we usually conducted [10–12]. The purity of the protein samples was verified by SDS–PAGE, and their molecular weights were confirmed using a Voyager STR matrix-assisted laser desorption ionization time-of-flight mass spectrometer (Applied Biosystems).

2.2. Circular dichroism (CD) spectroscopy and titration calorimetry (ITC)

All circular dichrosim (CD) experiments were performed on a Jasco J-810 spectropolarimeter as we previously described [10–12].

ITC was used to characterize the binding of three peptides with the catalytic domain of PAK4 with a Microcal VP ITC machine (GE). The catalytic domain was placed in a 1.4 ml sample cell while the peptides were loaded into a 300 μL syringe. The titration data were fitted by using the built-in software ORIGIN to obtain thermodynamic binding parameters as we conducted on other proteins [12].

2.3. NMR experiments

All NMR experiments have been performed at 25 °C on an 800 MHz Bruker Avance spectrometer. For sequential assignment, a ^{15}N-labeled NMR sample of the full-length regulatory domain (9–68) at a protein concentration of 500 μM was prepared in 10 mM sodium phosphate buffer (pH 6.3) in the presence of 10 mM dithiothreitol (DTT) and 10% D_2O for NMR spin-lock. Three-dimensional NMR ^{15}N-edited HSQC-TOCSY and HSQC-NOESY spectra were acquired and the subsequent analysis led to the sequential assignment. NOE connectivities were derived from HSQC-NOESY spectrum.

For HSQC titrations, NMR samples of three ^{15}N-labeled peptides at protein concentrations of 200 μM were prepared in 10 mM sodium phosphate buffer (pH 6.3) in the presence of 5 mM DTT and the catalytic domain was dialyzed to the same buffer. The two-dimensional NMR ^{1}H–^{15}N HSQC spectra were collected for three peptides in the absence and in the presence of the unlabeled

catalytic domain at molar ratios of 1:0.5, 1:1, 1:1.5 and 1:2 (peptide:catalytic domain). The disappeared/shifted residues were identified by superimposing HSQC spectra as we performed previously [12].

2.4. Crystallization and structural determination

The catalytic domain was prepared at a concentration of 6 mg/ml and mixed with the peptide at molar ratio 1:2 for crystallization, using hanging drop method at room temperature. The crystal was gained under the well with the reservoir solution 0.1 M TRIS, pH 8.5, 12% (M/V) PEG8000 for 3 days. The X-raydiffraction data for two crystals were collected with an in-house Rigaku/MSC FR-E X-ray generator with a Saturn 944 CCD detector, with a resolution of 2.8 Å. The details of structure determination and analysis have been described in Supplementary material.

3. Results

3.1. Residue-specific solution conformation of the N-terminal regulatory domain

We first characterized the solution conformation of the N-terminal regulatory domain over Val9-Lys68 of PAK4, which is sufficient to achieve the PAK4 auto-inhibition and to bind Cdc42/Rac [7]. As judged from its far-UV spectrum with the maximal negative signal at 201 nm (Fig. 1B), the domain is predominantly unstructured in the free state, without any stable secondary structures [10,11,14]. Furthermore, it is also lacking of any tight tertiary packing as evident from its HSQC spectrum which has narrow spectral dispersions on both ^{1}H and ^{15}N dimensions (Fig. 1C) [10,11,14].

Nevertheless, we succeeded in achieving its sequential assignment by analyzing HSQC-TOCSY and HSQC-NOESY spectra. Fig. 1D presents ^{1}H chemical shift deviations (CSD) from their corresponding random-coil values, which represents a powerful probe for detecting residual secondary structures in unfolded or partially folded proteins [13]. Small ^{1}H CSD values of all residues provide residue-specific evidence that consistent with the above CD and NMR results, this domain is indeed predominantly unstructured. Nevertheless, many residues have negative CSD values, indicating that these residues have weakly-populated helical/loop conformations, in particular over Asn16-Thr23 and Arg37-Lys51. The conclusion is further supported by the NOE pattern defining secondary structures (Fig. 1E). Strikingly, $d_{NN(i,i+2)}$ NOEs were also identified over Gln38-Arg48, suggesting that dynamic helical conformation is indeed populated over this region.

Recently a crystal structure (pdb: 2OV2) was deposited for the complex between the human Rac3 and the N-terminal regulatory region (Glu10-Leu42) of the human PAK4. In the structure, the residues Ser15-Asp26 and Gln30-Thr33 form two β-strands which are closely packed against the Rac3 structure. Based on the positive CSD values for residues Gln30-Lys32 (Fig. 1D), it seems that even in the free state, this region already has weakly-populated β-strand/extended conformation. By contrast, residues Asn16-Phe25 assuming a long β-strand in the complex structure have negative ^{1}H CSD values in the free state, which is an unambiguous indicator for a helical or loop conformation. This observation suggests that the region over Asn16-Phe25 is a chameleon sequence capable of forming different secondary structures in differential contexts, as previously observed on other proteins [11]. It is also worthwhile to point out that residues Gln38-Leu42 outside of the CRIB region also bind Rac3 to form a short helix. In fact, these residues have been previously shown to be part of AID [7].

3.2. Identification of the entire AID sequence

We subsequently attempted to identify the complete sequence of AID by monitoring the shift/disappearance of HSQC peaks of the ^{15}N-labeled regulatory domain (9–68) upon gradually adding the unlabeled PAK4 catalytic domain. As the chemical shift and intensity of NMR HSQC peaks are very sensitive to minor perturbations in chemical microenvironment of the NMR sensitive atomic nuclei (^{1}H and ^{15}N here), HSQC titration can detect much weaker protein–protein/peptide, protein–ligand interactions [12–14] than many other biophysical methods such as ITC which gives thermodynamic parameters of the binding under equilibrium by detecting the heat change associated with the binding event [12]. While unaffected HSQC peaks unambiguously indicate that their corresponding residues are not affected by binding, the shift/disappearance of the peaks could result from either direct binding contacts, or/and binding-induced conformational/dynamic changes of the corresponding residues, or both. As seen in Fig. 2A and B, upon adding the catalytic domain, many HSQC peaks of the ^{15}N-labeled regulatory domain were affected whose corresponding residues aremapped to be all located in the speculated AID [7] except for Gly34-Leu35 in CRIB. On the other hand, ITC characterization failed to detect any significant heat change during titrations (Fig. 2C). This phenomenon results from small heat changes undetectable by ITC, which is commonly observed for many binding interactions involved in intrinsically-unstructured proteins [14], either due to the weak binding, or/and despite being very rare, no significant heat change associated with the binding.

We subsequently generated a 33-residue peptide (29–61) covering all affected residues and found it to be unstructured as the full-length regulatory domain based on CD (Fig. 1B) and NMR HSQC spectra (Fig. 1C). Subsequently we characterized its binding with the catalytic domain by HSQC titrations, and the same set of residue was involved in binding the catalytic domain (Fig. 2A and D). Strikingly, ITC characterization detected a significant heat release and consequently its dissociation constant (Kd) could be fitted out to be 1.23 μM (Fig. 2E). This result together with the ITC result on the full-length regulatory domain (Fig. 2C) suggests that the presence of unstructured and binding-unnecessary residues would significantly reduce the binding affinity or/and attenuate the heat change associated with the binding, as we previously observed on other intrinsically-unstructured proteins [14]. To assess whether the disappearance of the Gly34-Leu35 HSQC peak was due to the direct contact or binding-induced conformational/dynamic changes, we further generated a 25-residue peptide (36–60) with Gly34-Leu35 and other unaffected residues deleted. Interestingly, its solution conformation remains similarly unstructured as the full-length one by CD and NMR spectroscopy (Fig. 1B and C). NMR titrations indicate that despite the removal of Gly34-Leu35, the remaining residues bind to the catalytic domain in the same way (Fig. 2F and A). Remarkably, ITC characterization showed that this peptide had a ~4-fold higher binding affinity than the 33-residue peptide, with a Kd of 320 nM (Fig. 2G). These results imply that the disappearance of Gly34-Leu35 peaks is most likely due to the binding-induced conformational/dynamic changes as extensively observed in other system [12,14]. Therefore, the 25-residue peptide (36–60) most likely contains all residues required for binding the PAK4 catalytic domain.

3.3. Crystal structures of the catalytic domain in complex with the entire AID

Previously, several forms of PAK4 with differentially-truncated N-terminal regions have been subjected to crystallization and subsequent structure determination [9], but the electron density could only be observed for a 6-residue pseudosubstrate motif over

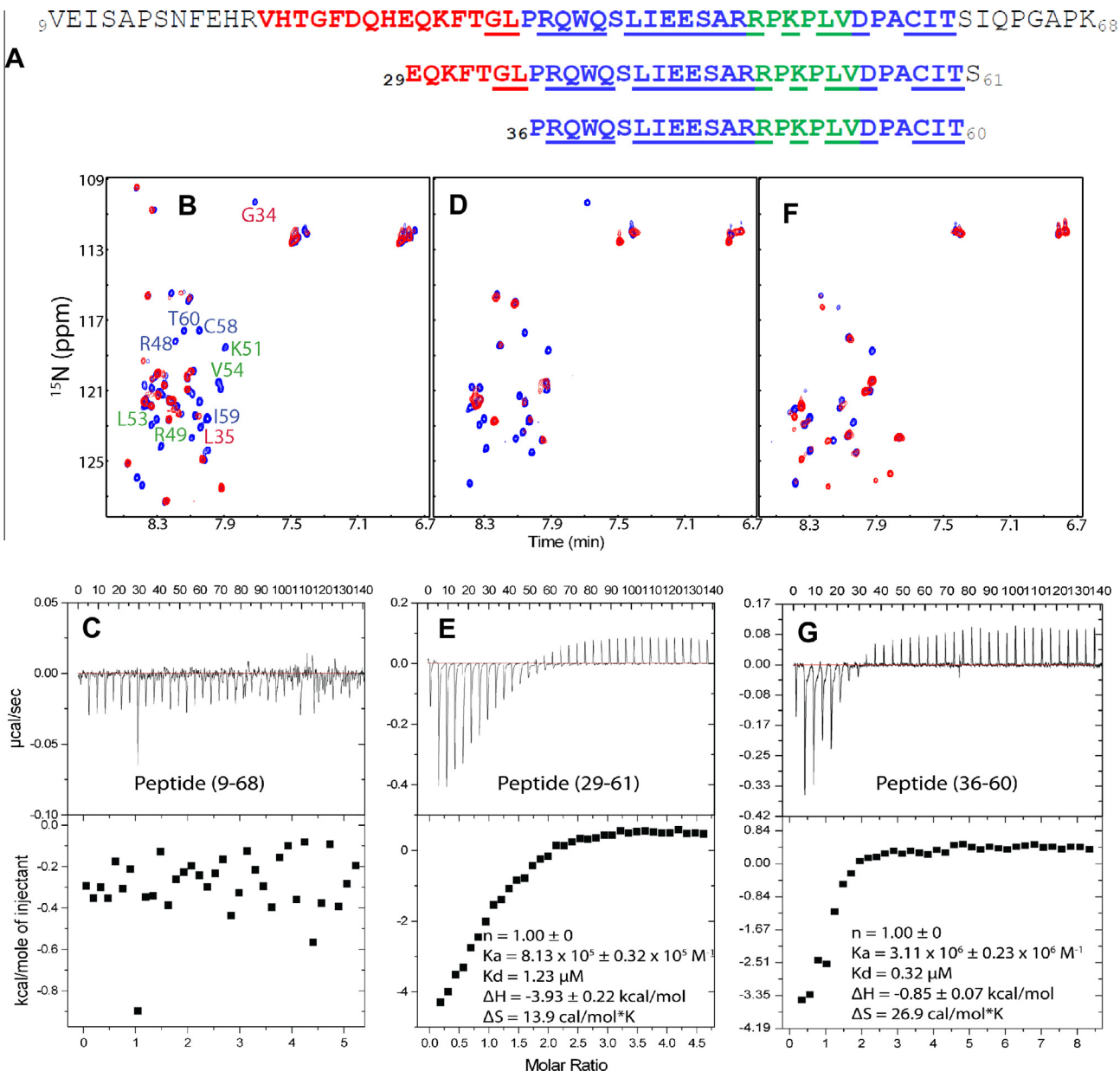

Fig. 2. Identification of the entire AID sequence. (A) Amino acid sequences of three peptides with binding-involved residues underlined. The CRIB residues are colored in red, AID residues in blue, pseudosubstrate residues in green and the rest in black. HSQC titrations of the unlabeled PAK4 catalytic domain into the ^{15}N-labeled peptides 9–68 (B), 29–61 (D) and 36–60 (F). For clarity, only HSQC spectra of the peptides in the absence of (blue) and in the presence of the catalytic domain (red) at a molar ratio of 1:2.0 (peptide:Cat) are superimposed. Some significantly affected HSQC peaks are labeled with their corresponding residues. ITC profiles of the binding reactions (top) of the PAK4 catalytic domain with the peptides 9–68 (C), 29–61 (E) and 36–60 (G), and integrated values for reaction heats with subtraction of the corresponding blank results normalized by the amount of ligand injected vs the molar ratio of the catalytic domain/peptide (bottom). The thermodynamic binding parameters obtained from fitting the data are shown. (For interpretation of the references to color in this figure legend, the reader is referred to the web version of this article.)

Arg49-Val54. So how is it possible that many more residues have been identified here to be required for binding the PAK4 catalytic domain but on the other hand, only six residues were visible in the complex structures? We believe that this is mostly due to the facts that in theprevious constructs, there still existed a large portion of unstructured and binding-unnecessary residues, or/and some AID residues were deleted, either of which would result in the reduction of the binding affinity, or/and intervention in crystallization/diffraction.

Indeed, we co-crystallized the PAK4 catalytic domain in complex with the 25-residue peptide. The crystal was identified as belonging to the space group $P4_12_12$ with $a = 65.175$, $b = 65.175$, $c = 184.567$, $\alpha = \beta = \gamma = 90°$ and the structure has been determined at a resolution of 2.8 Å by molecular replacement with the previously-determined structure (4FIJ) [9]. The electron density is visible for the backbones of 20 residues Trp39-Cys58 as well as side chains of Arg48, Arg49, Pro50, Pro52, Leu53 and Asp55. Supplementary Table S1 presents the refinement statistics for the structure determination and the structure was deposited in the RCSB Protein Data Bank with the RCSB ID code rcsb080231 and PDB ID code 4L67.

Fig. 3A presents the complex structure at a 2.8 Å resolution, in which residues 300–589 are visible for the PAK4 catalytic domain and 20 out of 25 residues can be seen for AID. Like all structures previously determined for thePAK4 catalytic domain, Ser474 is also phosphorylated in the present structure. Strikingly, the present

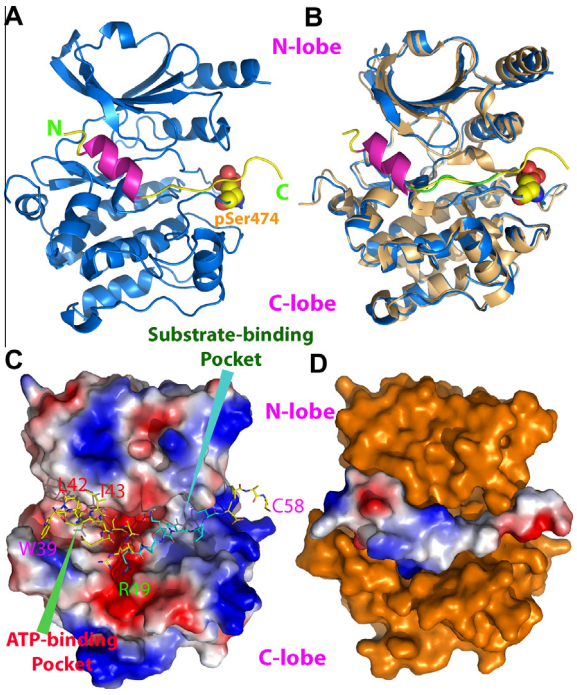

Fig. 3. Crystal structures of the PAK4 catalytic domain in complex with the entire AID. (A) Crystal structure at 2.8 Å of the PAK4 catalytic domain (blue) in complex with the entire AID with the helix over Trp39-Arg48 in pink and rest in yellow. Phosphorylated Ser474 is displayed in spheres. (B) Superimposition of the present structure (blue) with 4FII [9] (light brown) containing a 6-residue pseudosubstrate motif Arg49-Val54 (green). (C) The electrostatic potential surface of the PAK4 catalytic domain in complex with the 20-residue AID residues displayed in sticks, with cyan to indicate the backbones of 6-residue pseudosubstrate motif previously observed (4FII), and rest in yellow. (D) The PAK4 catalytic domain displayed in brown surface in complex with AID in the electrostatic potential surface. (For interpretation of the references to color in this figure legend, the reader is referred to the web version of this article.)

structure of the PAK4 catalytic domain including the activation loop with phosphorylated Ser474 is almost identical to that in the fully active state (pdb: 4FIJ) [9], with a backbone RMS deviation of only 0.60 Å; in complex with the pseudosubstrate motif (pdb: 4FII) [9], with a backbone RMS deviation of only 0.61 Å; the full-length PAK4 (pdb: 4FIE) [9], with a backbone RMS deviation of only 0.69 Å, as well as in complex with aspecific PAK4 inhibitor PF-3758309 (pdb: 2X4Z) [15], with a backbone RMS deviation of only 0.79 Å. This observation strongly suggests that no significant structural changes occur for the PAK4 catalytic domain to transform from the inactivated to activated states.

The most striking feature observed in the present structure is that upon binding the PAK4 catalytic domain, the unstructured AID residues insert into the kinase cleft and transform into an N-terminal α-helix over residues Trp39-Arg48 and a pseudosubstrate motif over residues Arg49-Val54. Interestingly, the pseudosubstrate motif which has been previously observed to occupy the substrate-binding pocket [9], has a conformation very similar to the corresponding residues in the present AIDstructure (Fig. 3B). Moreover, in the present structure, four extra residues Asp55-Cys58 are observed at the C-terminus of the pseudosubstrate motif, which have a hydrogen bond between the backbone CO atom of the AID Asp55 and guanidinium atom of Arg359. Moreover, the guanidinium atom of the AID Arg49 forms salt bridges with carboxylate atoms of both Glu507 and Asp444. As such, the side chain of the AID Arg49 deeply inserts into a very negatively-charged pocket in the kinase cleft (Fig. 3C). Remarkably, the N-terminal 10 residues Trp39-Arg48, which is highly unstructured with only a weakly-populated helical conformation in the free state (Fig. 1), fold into well-formed α-helix upon inserting into the kinase cleft. This transformation is usually called the binding-induced/coupling folding, which is characteristic ofintrinsically unstructured proteins [16]. This characteristic AID helix has close contacts with the glycine-rich loop of the catalytic domain, which is critical for binding ATP. For example, there are hydrogen bonds between the sidechain O atom of the AID Ser46 with the backbone NH atom of Lys326. Furthermore, the hydrophobic side chains of the AID Leu42 and Ile43 closely contact the hydrophobic patches over the ATP-binding pocket (Fig. 3C). Interestingly, as shown in Fig. 3D, the 20-residue AID has a complimentary electrostatic potential surface which occupies the complete kinase cleft including substrate- and ATP-binding pockets, thus physically rendering the kinase cleft to be inaccessible to both substrate and ATP.

4. Discussion

Recently, PAK4 including other group II PAKs has been emerging as key targets for design of anti-tumor drugs [7–9,15,17,18]. Indeed, a specific PAK4 inhibitor (PF-3758309) has shown efficacy in mouse models of cancer [15]. These results suggest a promising potential for developing group II PAK inhibitors for treating tumors. Therefore, a mechanistic understanding of how group II PAK activity is auto-inhibited represents an essential and critical step for delineating their roles in physiology as well as for further developing potent and specific therapeutics.

In the present study, we first experimentally demonstrate that the N-terminal regulatory domain sufficient for auto-inhibiting PAK4 and binding Cdc42 isintrinsically unstructured. Nevertheless, NMR HSQC titrations lead to the identification of the entire AID sequence and subsequently by removing unstructured and binding-unnecessary residues, we obtained a 25-residue AID peptide which shows a high binding affinity, with a Kd of 320 nM, to the PAK4 catalytic domain. Most strikingly, this success allowed our determination of the crystal structure of the PAK4 catalytic domain in complex with the entire AID, which reveals that the AID residues occupies the complete kinase cleft by a newly-observed N-terminal helix as well as a previously-identified pseudosubstrate motif, thus achieving the auto-inhibition.

Our results clearly decipher that the auto-inhibition mechanisms for PAK4 and PAK1 are completely different in three ways. Firstly, although the N-terminal regulatory domain of PAK1 is also unstructured [5,18], upon binding the PAK1 catalytic domain, it folds into a well-packed structure in the dimeric form (Fig. 4A), composed of both AID and CRIB regions [5]. By contrast, upon binding the PAK4 catalytic domain, only the AID residues of the N-terminal regulatory domain of PAK4 undergo structural rearrangements characteristic of the formation of a N-terminal helix (Fig. 4C), while most CRIB residues remains unaffected and unstructured as evidenced by the NMR characterization. Secondly, for PAK1, the N-terminal domain is mostly packed against the C-lobe of the catalytic domain and only an inhibitory tail Ser139-Asp147 occupies the substrate-binding pocket of the kinase cleft as a pseudosubstrate (Fig. 4B), which also displaces the activation loop into a disorder state. By contrast, the PAK4 AID appears to auto-inhibit the kinase by physically blocking the complete kinase cleft which has no significant perturbation on the structure of the activation loop, with a 6-residue pseudosubstrate motif occupying the substrate-binding pocket and a 10-residue helix binding the rest of the cleft, including the ATP-binding pocket (Fig. 4D). Thirdly, upon activation, significant structural rearrangements occur for the PAK1 catalytic domain, in particular over the activation loop [5]. By contrast, no significant structural difference has been observed for all available structures of the PAK4 catalytic domain in the activated and inhibited states. Therefore, the PAK4 auto-inhibi-

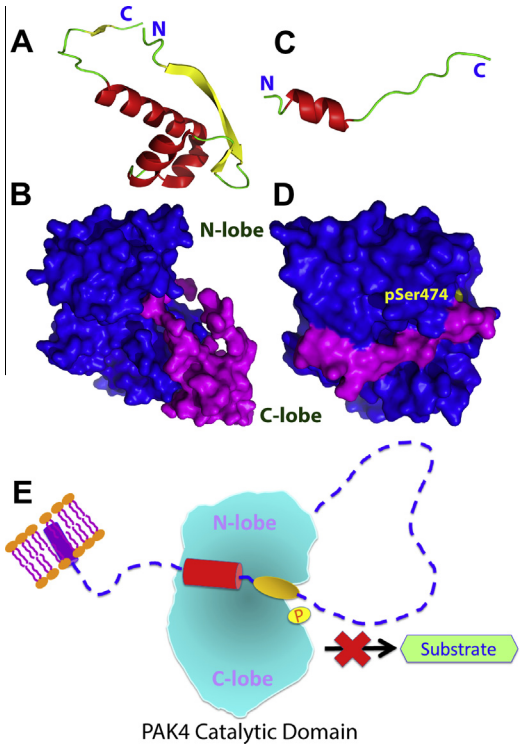

Fig. 4. Different auto-inhibition mechanisms for PAK1 and PAK4. (A) The bound structure of the PAK1 N-terminal regulatory domain in the monomeric form isolated from the crystal structure 1F3M [5]. (B) Surface representation of the PAK1 catalytic domain (blue) in complex with its N-terminal regulatory domain (pink) in the monomeric form. (C) The bound structure of the PAK4 AID as determined in the present study. (D) Surface representation of the PAK4 catalytic domain (blue) in complex with its AID (pink). (E) Schematic representation of the PAK4 catalytic domain (cyan body) auto-inhibited by its AID composed of a characteristic helix over Trp39-Arg48 (red cylinder) and a pseudosubstrate motif (yellow ellipsoid) in the N-terminal regulatory domain which is anchored onto the membrane by NLS. (For interpretation of the references to color in this figure legend, the reader is referred to the web version of this article.)

tion appears to be mostly achieved by the physical occupancy of the complete kinase cleft with AID, thus blocking the substrate and ATP to access the catalytic machinery hosted inthe kinase cleft (Fig. 4E). Intriguingly, in the crystal structure of the human Rac3 in complex with the PAK4 CRIB domain (2VO2), the PAK4 residues Gln38-Leu42, which also constitute the N-half of the characteristic AID helix occupying the PAK4 kinase cleft as disclosed here, form a short helix and are closely packed against the Rac3 structure. This implies that Cdc42/Rac and PAK4 catalytic domain may compete in binding this characteristic helix. Therefore, in the future, it would be of significant interest to define that to which degree Cdc42/Rac-binding affects the auto-inhibition of PAK4.

As three group II PAKs share high sequence homology and functional similarity [7–9], it is highly likely that PAK5 and PAK6 may also be regulated by the similar mechanism observed here for PAK4. Our study reveals that PAK4 and PAK1 have differentmechanisms for their auto-inhibition, thus implying a strategy to design specific inhibitors for PAK4 starting from the entire AID sequence, namely to chemically modifying AID to transform it to non-peptide molecules but in the meanwhile to retain, or even enhance the affinity and specificity towards PAK4, as previously conducted on the PAK1 AID [18] and thrombin inhibitors [19].

Acknowledgments

This study is supported by Ministry of Education (MOE) of Singapore Tier 2 grant MOE2011-T2-1-096 to J. Song. W. Wang is a recipient of the MOE graduate scholarship under theMOE grant R-154-000-388-112 to J. Song. We would thank Dr. Jobichen Chacko at Department of Biological Sciences, National University of Singapore; and Dr. Sundramurthy Kumar at Biomedical Sciences Institutes (BMSI), A*STAR, for their assistance in collecting and analysing X-ray diffraction data.

Appendix A. Supplementary data

Supplementary data associated with this article can be found, in the online version, at http://dx.doi.org/10.1016/j.bbrc.2013.07.047.

References

[1] G.M. Bokoch, Biology of the p21-activated kinases, Annu. Rev. Biochem. 72 (2003) 743–781.
[2] Z.S. Zhao, E. Manser, PAK and other Rho-associated kinases-effectors with surprisingly diverse mechanisms of regulation, Biochem. J. 386 (2005) 201–214.
[3] C.M. Wells, G.E. Jones, The emerging importance of group II PAKs, Biochem. J. 425 (2010) 465–473.
[4] L.E. Arias-Romero, J. Chernoff, A tale of two Paks, Biol. Cell 100 (2008) 97–108.
[5] M. Lei, W. Lu, Structure of PAK1 in an autoinhibited conformation reveals a multistage activation switch, Cell 102 (2000) 387–397.
[6] A. Abo, J. Qu, M.S. Cammarano, et al., PAK4, a novel effector for Cdc42Hs, is implicated in the reorganization of the actin cytoskeleton and in the formation of filopodia, EMBO J. 17 (1998) 6527–6540.
[7] Y. Baskaran, Y.W. Ng, W. Selamat, et al., Group I and II mammalian PAKs have different modes of activation by Cdc42, EMBO Rep. 13 (2012) 653–659.
[8] J. Eswaran, W.H. Lee, J.E. Debreczeni, et al., Crystal Structures of the p21-activated kinases PAK4, PAK5, and PAK6 reveal catalytic domain plasticity of active group II PAKs, Structure 15 (2007) 201–213.
[9] B.H. Ha, M.J. Davis, C. Chen, et al., Type II p21-activated kinases (PAKs) are regulated by an autoinhibitory pseudosubstrate, Proc. Natl. Acad. Sci. USA 109 (2012) 16107–16112.
[10] M. Li, J. Song, The N- and C-termini of the human Nogo molecules are intrinsically unstructured: bioinformatics, CD, NMR characterization, and functional implications, Proteins 68 (2007) 100–108.
[11] J. Liu, J. Song, NMR evidence for forming highly populated helical conformations in the partially folded hNck2 SH3 domain, Biophys. J. 95 (2008) 4803–4812.
[12] H. Qin, J. Shi, R. Noberini, et al., Crystal structure and NMR binding reveal that two small molecule antagonists target the high affinity ephrin-binding channel of the EphA4 receptor, J. Biol. Chem. 283 (2008) 29473–29484.
[13] H.J. Dyson, P.E. Wright, Unfolded proteins and protein folding studied by NMR, Chem. Rev. 104 (2004) 3607–3622.
[14] G. Gupta, H. Qin, J. Song, Intrinsically unstructured domain 3 of hepatitis C Virus NS5A forms a "fuzzy complex" with VAPB-MSP domain which carries ALS-causing mutations, PLoS One 7 (2012) e39261.
[15] B.W. Murray, C. Guo, J. Piraino, et al., Small-molecule p21-activated kinase inhibitor PF-3758309 is a potent inhibitor of oncogenic signaling and tumor growth, Proc. Natl. Acad. Sci. USA 107 (2010) 9446–9451.
[16] H.J. Dyson, P.E. Wright, Intrinsically unstructured proteins and their functions, Nat. Rev. Mol. Cell Biol. 6 (2005) 197–208.
[17] Z.S. Zhao, E. Manser, Do PAKs make good drug targets? F1000, Biol. Rep. 2 (2010) 70.
[18] R.K. Jha, Y.I. Wu, J.S. Zawistowski, et al., Redesign of the PAK1 autoinhibitory domain for enhanced stability and affinity in biosensor applications, J. Mol. Biol. 413 (2011) 513–522.
[19] J. Song, F. Ni, NMR for the design of functional mimetics of protein-protein interactions: one key is in the building of bridges, Biochem. Cell Biol. 76 (1998) 177–188.